

## Temporal and spectral evolution of runaway electron bursts in TEXTOR disruptions

M. Forster, K. H. Finken, T. Kudyakov, M. Lehnen, O. Willi, Y. Xu, L. Zeng, and the TEXTOR Team

Citation: *Physics of Plasmas* **19**, 092513 (2012); doi: 10.1063/1.4755787

View online: <http://dx.doi.org/10.1063/1.4755787>

View Table of Contents: <http://scitation.aip.org/content/aip/journal/pop/19/9?ver=pdfcov>

Published by the AIP Publishing

---

### Articles you may be interested in

[Measurements of the runaway electron energy during disruptions in the tokamak TEXTOR](#)

*Phys. Plasmas* **19**, 052506 (2012); 10.1063/1.4717759

[Resistive stability of a plasma with runaway electrons](#)

*Phys. Plasmas* **14**, 122102 (2007); 10.1063/1.2817016

[Runaway electrons and the evolution of the plasma current in tokamak disruptions](#)

*Phys. Plasmas* **13**, 102502 (2006); 10.1063/1.2358110

[Nonlinear evolution of the  \$m = 1\$  internal kink mode in the presence of magnetohydrodynamic turbulence](#)

*Phys. Plasmas* **13**, 032506 (2006); 10.1063/1.2179772

[Nonlinear acceleration of the electron inertia-dominated magnetohydrodynamic modes due to electron parallel compressibility](#)

*Phys. Plasmas* **12**, 092505 (2005); 10.1063/1.2042167

---

Did your publisher get  
**18 MILLION DOWNLOADS** in 2014?  
AIP Publishing did.



THERE'S POWER IN NUMBERS. Reach the world with AIP Publishing.



# Temporal and spectral evolution of runaway electron bursts in TEXTOR disruptions

M. Forster,<sup>1,a)</sup> K. H. Finken,<sup>1</sup> T. Kudyakov,<sup>1</sup> M. Lehnen,<sup>2</sup> O. Willi,<sup>1</sup> Y. Xu,<sup>3</sup> L. Zeng,<sup>2,4</sup> and the TEXTOR Team<sup>2</sup>

<sup>1</sup>*Institut für Laser- und Plasmaphysik, Heinrich-Heine-Universität Düsseldorf, Universitätsstr. 1, 40225 Düsseldorf, Germany*

<sup>2</sup>*Institut für Energie- und Klimaforschung, Forschungszentrum Jülich GmbH, EURATOM Association, 52425 Jülich, Germany*

<sup>3</sup>*Laboratory for Plasma Physics, Ecole Royale Militaire-Koninklijke Militaire School, Avenue de la Renaissance 30, 1000 Brussels, Belgium*

<sup>4</sup>*Institute of Plasma Physics, Chinese Academy of Sciences, P.O. Box 1126, Hefei 230031, People's Republic of China*

(Received 11 July 2012; accepted 12 September 2012; published online 27 September 2012)

Novel observations of the burst-like runaway electron losses in tokamak disruptions are reported. The runaway bursts are temporally resolved and first-time measurements of the corresponding runaway energy spectra are presented. A characteristic shape and burst to burst changes of the spectra are found. The runaway energy content of the disruptions and the conversion of the predisruptive magnetic energy are estimated. The radial decay of the runaways can be approximated by an exponential distribution. Deriving from the measurements, resistive tearing modes or kink modes are suggested to trigger the formation of the bursts. © 2012 American Institute of Physics. [<http://dx.doi.org/10.1063/1.4755787>]

## I. INTRODUCTION

The free fall acceleration of electrons into the relativistic regime is known in various kinds of plasmas including astrophysical ones, thunderbolts and fusion plasmas as electron runaway. For future fusion reactors, especially reactor sized tokamaks, runaway electrons (RE)<sup>1</sup> are an issue of great importance. The tokamak disruption instability<sup>2,3</sup> can include the conversion of a substantial part of the plasma current into a RE current. When the high energetic RE are lost, they can strike the plasma facing components at localized spots. Due to their high energies up to a few tens of MeV, the RE can easily propagate through several cm of low atomic number material and even melt high atomic number material on the surface.<sup>4</sup> For ITER,<sup>5</sup> an inherent susceptibility for efficient plasma current conversion into a RE current of up to 70% is expected. A RE content of 50 MJ in ITER disruptions as well as resulting peak energy depositions enough to melt or ablate the ITER wall materials are predicted.<sup>6</sup> Consequently, RE carry the potential to reduce the lifetimes of wall components and even destroy sensitive, i.e. actively cooled parts.<sup>7</sup>

The research for an effective suppression of the RE generation<sup>8–12</sup> is hampered by the lack of a complete understanding of the RE evolution during disruptions. X-ray measurements<sup>13,14</sup> indicate the loss of RE in disruptions in form of pulses shorter than a ms. In this letter, we present novel results of a scintillation detector measurement at the plasma edge of the tokamak TEXTOR (major radius  $R = 1.75$  m, minor radius  $a = 0.46$  m). There is only limited spectral information about RE in disruptions in the literature. It stems for example from synchrotron radiation measurements<sup>12</sup> of RE with energies larger than 25 MeV, from the

detection of neutrons<sup>15,16</sup> produced in photonuclear reactions after the deceleration of electrons with energies larger than 10 MeV and from previous probe measurements.<sup>17</sup> This letter reports on temporally and spectrally resolved observations of the RE bursts and a discussion of the physical loss mechanism responsible for the bursts. The experimental data enable an estimation of the RE energy content of the disruption and hence a discussion of the conversion efficiency of predisruptive, magnetic plasma energy into RE energy. From the measured RE spectra, a conclusion about the radial decay distribution of the RE can be drawn by a comparison with former probe studies.<sup>18</sup>

## II. EXPERIMENTAL SCENARIO

The disruptions in ohmic discharges with  $B_t = 2.4$  T,  $I_p = 350$  kA, and  $n_e = 1.5 \cdot 10^{19} \text{ m}^{-3}$  were induced by the injection of about 0.05 bar l of argon which corresponds to about  $10^{21}$  atoms. The valve was triggered 2 s after the start of the discharge.<sup>11</sup> This procedure guarantees the reliable generation of RE at TEXTOR. A fast movable mechanism inserted the scintillating probe described in Ref. 19 along the minor radius into the low field side (LFS) of the machine on an ms timescale. The probe was used to measure the RE directly at the plasma edge. The inner parts of the probe are shielded against particles and light from the plasma by a 5 mm thick graphite housing. Only RE with energies larger than 4 MeV can propagate through the housing and deposit their energy in the nine scintillating crystals. The produced light is guided by optical fibres to a set of photomultipliers. The setup has a RC loading time of about 30  $\mu\text{s}$  determining the temporal resolution. The crystals are shielded by different thicknesses of stainless steel against the electrons and hence detect different energy ranges giving the probe a

<sup>a)</sup>Electronic mail: Michael.Forster@uni-duesseldorf.de.

spectral resolution as well. The probe was absolutely calibrated using well defined monoenergetic electron beams provided by the electron accelerator ELBE at Forschungszentrum Dresden Rossendorf. Comparison of the experimentally observed energy deposition of the electrons with Geant4 simulations<sup>4</sup> shows an agreement within 50%. This determines the accuracy of the spectral resolution. The contribution of Bremsstrahlung and neutrons to the probe signal were found to be negligible during TEXTOR shots. In the presented experimental campaign, the probe was inserted 300 ms before the gas injection and it remained at the position until about 250 ms after the injection. The radial position of measurement was scanned from 48.5 to 47 cm from shot to shot in 5 mm steps. Before the disruption, the last closed magnetic flux surface is determined by the toroidal belt limiter at the minor radius of 46.3 cm. The exact position of the RE beam is not monitored but the vertical field coils of TEXTOR are used to deflect the beam via feed forward control to the LFS where the probe is inserted.

### III. MEASUREMENTS OF THE RUNAWAY ELECTRON BURSTS

Fig. 1 displays temporal signals of a typical disruption of the campaign. The disruption starts with the negative spike in the loop voltage at 2.0044 s, seen in Fig. 1(a), followed by a drop of the electron temperature  $T_e$  (thermal

quench) seen in the electron cyclotron emission (ECE) in Fig. 1(b). The measured frequencies of 133 to 148 GHz correspond to a resonance at a major radius of 1.59 m. The signal does not go to zero, rather it drops to about 30% as the ECE does not provide an absolute measurement of  $T_e$  under the given conditions. It gives a measurement of the radiation temperature which is enough to monitor the generation of RE with energies below 3 MeV.<sup>11</sup> The acceleration of electrons into the runaway regime is induced by the steep rise of the loop voltage to almost 40 V. The ECE shows a gradual increase, due to suprathermal synchrotron radiation, although the plasma is cold. After the thermal quench, the plasma current starts to decay exponentially (current quench). This is retarded by the practically collisionless RE which form one or more current plateaus. In Fig. 1(c), the successive formation of 3 RE plateaus is indicated by the arrows. When a plateau starts to decay, the RE are expelled from the plasma and seen by the probe at  $r=47.5$  cm as the bursts shown in Fig. 1(d). Simultaneously, the Mirnov coil signal in Fig. 1(e) shows a spiked magnetic activity with a temporal resolution of about 5  $\mu$ s. During the second plateau the ECE shows a peak, which indicates the generation of RE, which are then also detected by the probe. During the third plateau, the probe does not measure any RE losses and the ECE is at the level of noise. In contrast, the soft x-rays detected by viewing along a central line of sight and shown in Fig. 1(f) indicate an interaction of RE with the background plasma. Hence, it is not clear if this current is purely thermal or also carried by RE. Fig. 2(a) shows the temporal evolution of the RE probe signal in different spectral ranges for the shaded region in Fig. 1. Integrating the 3 peaks of Fig. 2(a), respectively, and using the calibration of the probe leads to the absolute energy spectra of the measured RE as seen in Fig. 2(b). The spectrum of the first peak is exponentially decaying towards higher energies except for a small deviation from this behaviour around 15 MeV. Moreover, the spectra show changes. From burst 1 to 2, the fraction of RE with energies around 6 MeV decreases and from burst 2 to 3, the fraction around 15 MeV increases to a considerable enhancement. The spectra and their burst to burst changes presented in Fig. 2(b) are similarly observed throughout the campaign. All the RE spectra which were measured at the minor radius of 47.5 cm are shown in a histogram in Fig. 3. It can be seen that the shape of the spectrum, especially the enhancement around 15 MeV, is reproduced during the 7 disruptions. About 93% of the 46 RE spectra measured during 17 disruptions at 4 different radial positions show a deviation from an exponential decay around 15 MeV. Consequently, this shape must be seen as a general characteristic of the spectra of the RE in TEXTOR disruptions. The spectra in Fig. 2(b) contain only the number of RE detected by the probe crystals. From the RE current, the total number of RE in the disruption and hence a scaling factor for the burst spectra to contain all the RE is calculated. The application of this scaling factor is justified because the measurements have shown that the spectra are independent of the radial probe position. Thus, if RE bursts strike the probe partly, the undetected parts are assumed to have the same spectra as the detected ones. The spectra of the bursts which completely

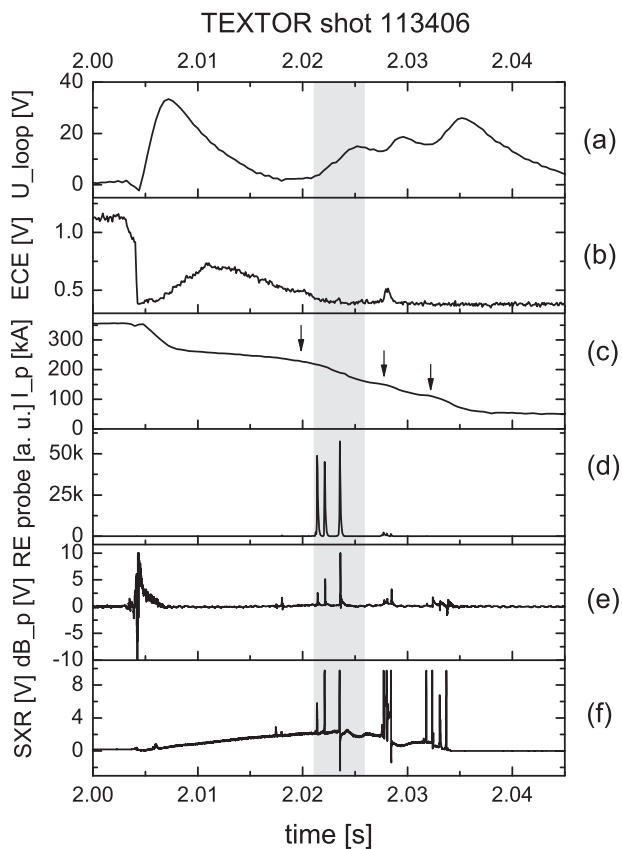
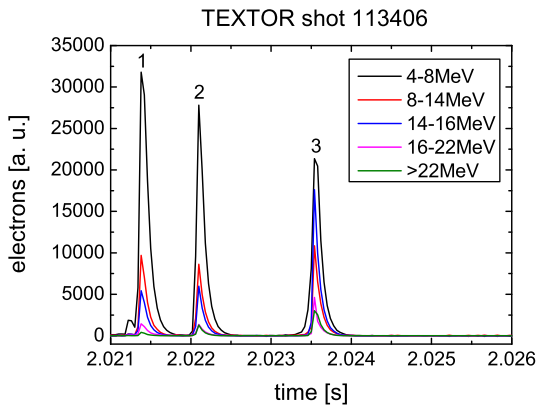
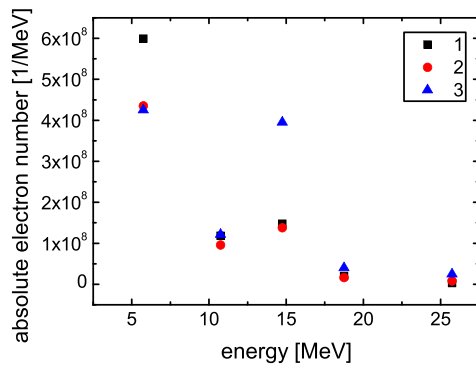


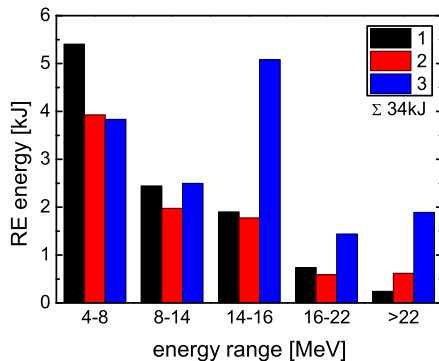
FIG. 1. For a typical disruption the temporal evolution of (a) the loop voltage, (b) the ECE, (c) the plasma current with 3 arrows indicating RE plateaus, (d) the probe signal showing RE with energies  $>4$  MeV, (e) the signal of a Mirnov coil on the LFS and (f) soft X-rays detected along a central line of sight are presented.



(a) Temporally and spectrally resolved RE bursts



(b) Energy spectra in the 3 bursts



(c) Total RE energy in the 3 bursts

FIG. 2. RE probe measurement at 47.5 cm radius during the same disruption as in Fig. 1.

miss the probe should not differ too much in the contained total energy as the burst to burst changes in the measured spectra indicate. The scaling procedure leads to Fig. 2(c). The energy content in kJ is shown for each of the 3 bursts. Most of the RE energy is contained in the range of particles with 4 to 8 MeV although the energy drops from burst to burst. An increase is seen in the RE energy in the spectral range between 14 and 16 MeV. A substantial part of the energy is carried by these electrons. The RE fraction with energies above 22 MeV contains a few kJ. The total RE energy is about 34 kJ. Fig. 4 shows the poloidal magnetic

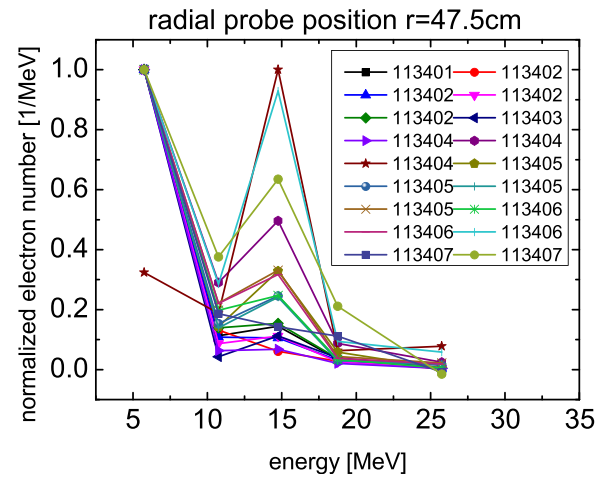


FIG. 3. Histogram of the RE energy spectra measured by the scintillator probe at 47.5 cm minor radius during 7 disruptions.

activity, seen in Fig. 1(e), in more detail. The oscillations grow on a timescale of  $\tau_{osc} \approx 40 \mu s$ . The spikes 1 to 3 correspond to the RE bursts 1 to 3 in Fig. 2(a).

In order to give a complete overview of the RE evolution in the disruptions analyzed in this letter, data from another discharge is used to show that a continuous onset of RE losses during the decay of the plasma current preceding the formation of the bursts as well as RE losses during the thermal quench can also occur. Fig. 5 shows a temporal comparison of the probe signal of RE with energies above 4 MeV (b) and the plasma current (a). From about  $t = 2.01$  to 2.03 s, the current plateau decreases slowly and continuous electron losses build up. Then a physical mechanism triggers much higher losses leading to a stronger decrease of the RE plateau and the bursts seen in the probe signal. The bursts stop before all the current has decayed. This can be either due to the conversion of RE current back to thermal current or the remaining current is carried by RE below the probe's detection threshold of 4 MeV. An arrow in Fig. 5(b) indicates a probe signal during the thermal quench. This is shown enlarged in Fig. 5(c). The signal shows RE losses

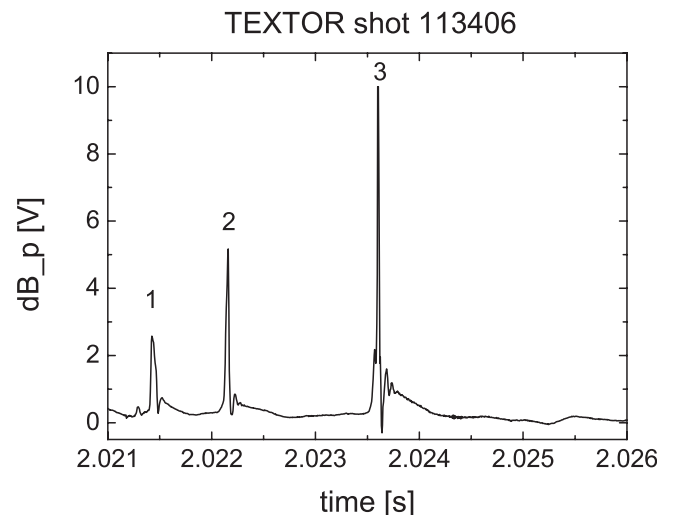


FIG. 4. Poloidal magnetic oscillations measured by a Mirnov coil on the LFS and corresponding to the 3 RE bursts in Fig. 2(a).



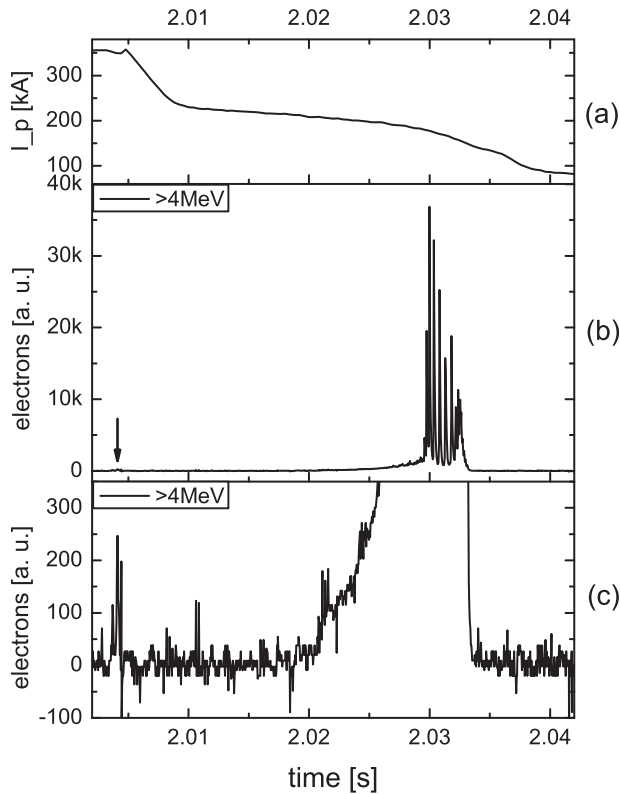


FIG. 5. Temporal evolution of (a) the plasma current, (b) the probe signal for RE with energies  $>4$  MeV and (c) enlarged, the probe signal during the thermal quench of a disruption; the arrow in (b) marks the RE losses during the thermal quench.

which are about 150 times smaller than the bursts during the current quench. These RE could stem from a population, which was produced prior to the disruption, e.g. during the start up of the discharge. The RE are accelerated to energies of up to 30 MeV at TEXTOR but the perturbation of the magnetic topology during the thermal quench affects the transport of the RE with energies between 4 and 6 MeV much more than that of the RE with higher energies.<sup>23</sup> This would explain the small signal which is only seen by the first probe channel. Another possible explanation is the generation of these RE at the onset of the disruption, triggered by the large electric field, via the Dreicer mechanism.

#### IV. PHYSICAL DISCUSSION OF THE RESULTS

Just 3 disruptions out of the 17 in the campaign show probe signals which indicate RE losses during the thermal quench. These losses are smaller than the bursts by factors of 12 to 150. The number of RE bursts during the current quench ranges from a few distinct bursts like in Fig. 1 to numerous bursts on a continuous pedestal like in Fig. 5. The widths of the bursts are in the range  $\tau_{FWHM} = 0.07$  to  $0.17$  ms. The delays between the bursts are  $\tau_d = 0.12$  to  $9.3$  ms. The period of RE losses during the current quench spans a range of  $\tau_{loss} = 2$  to  $14$  ms. The first RE burst is seen 17 to 25 ms after the negative voltage spike. The height of the probe signal shows large variations from shot to shot because the RE beam does not always strike the probe fully or even misses it. This indicates a RE beam radius smaller than the

predisruptive plasma column which is in agreement with the increase of the internal inductance in RE plateau plasmas.<sup>20</sup> The typical delay between the RE bursts is 1 ms. A simple estimation of the acceleration of the electrons is done assuming the electrons to travel at the speed of light. The loop voltage is set to 40 V. Accordingly, the RE can gain less than 1 MeV from the electric field between the bursts. The burst to burst differences in the spectra cannot be explained by the acceleration of the electrons. The calculated total RE energy ranges from 29 to 46 kJ which agrees very well with the measurements in Ref. 21. The predisruptive, magnetic energy is calculated as  $E_{mag} = \frac{1}{2} I_p^2 L_p$  with the inductivity  $L_p = \mu_0 R [\ln(8R/a) - 2 + \ell_i/2]$ . Using the typical internal inductance  $\ell_i = 1.2$  of TEXTOR prior to disruptions, the conversion of magnetic into RE energy is calculated to be between 11 and 17%. Assuming an exponential energy spectrum, one obtains an e-folding energy of around 9 MeV. The RE heat load probe experiment in Ref. 18 delivered an exponential radial decay of the RE beam for e-folding energies of 3.7 to 9.1 MeV and a linear radial decay for e-folding energies of 3.2 to 6.25 MeV. Comparing the results of the two experiments, provides a strong evidence for an exponential radial distribution of the RE. Evaluating the temporal properties of the RE bursts and the magnetic oscillations, allows a discussion of the physical mechanism which triggers the RE losses. Principally, the magnetic activity, which is measured simultaneously to the RE bursts, can be caused by two kinds of instabilities. Ideal kink instabilities of the RE beam would grow on an Alfvén timescale with  $\tau_A = R/(B_t/(\mu_0 n_i m_i)^{1/2}) \approx 1 \mu s$ . This is much faster than the observed half widths of the RE bursts or the growth times  $\tau_{osc}$  of the magnetic oscillations. The second possibility, which is theoretically suggested in Ref. 22, is the presence of resistive tearing modes in the background plasma. Due to the suprathermal nature of the radiation, no temperature measurements are available during the postdisruptive phase. As the main material of TEXTOR is graphite, which radiates strongly during the disruption, one can reasonably assume  $T_e \approx 10$  eV during the current quench. Thus, the resistive diffusion time reads  $\tau_R = \mu_0 a^2 / \eta \approx 2$  ms. This matches well the rearrangement of the current profile during the delay  $\tau_d$  between the bursts. The growth time of the tearing modes  $\gamma^{-1} \approx \tau_R^{3/5} \tau_A^{2/5} \approx 100 \mu s$  is close to  $\tau_{osc}$  and the half widths of the RE bursts. In a study<sup>23</sup> of the RE transport due to resonant magnetic perturbations in stationary TEXTOR discharges, similar RE spectra are measured. The presence of magnetic islands inside the plasma is shown by simulations. Their influence on the transport is found to cause the RE spectra with the bump around 15 MeV. Because of the lack of a  $T_e$ -profile measurement during the current quench, the formation of tearing modes cannot be proven. Thus, tearing and kink modes are the candidates which might trigger the RE bursts.

#### V. SUMMARY

In summary, we presented the first temporally and spectrally resolved analysis of RE bursts in tokamak disruptions. The bursts have temporal widths of 0.07 to 0.17 ms and they follow each other with delays of 0.12 to 9.3 ms. The energy

spectra in the bursts are approximately exponentially decaying except for an enhancement at around 15 MeV. The spectra show changes from burst to burst. The radial distribution of the RE is concluded to be exponential. The total RE energy in the disruptions is estimated to be between 29 and 46 kJ leading to a magnetic energy conversion of 11% to 17%. The RE energy is studied in more detail using a calorimeter probe designed for the RE.<sup>21</sup>

## ACKNOWLEDGMENTS

This work was funded by the GRK 1203, an F and E contract and the Trilateral Euregio Cluster (TEC).

- <sup>1</sup>P. Helander, L.-G. Eriksson, and F. Andersson, *Plasma Phys. Controlled Fusion* **44**, B247 (2002).
- <sup>2</sup>P. C. ITER Physics Expert Group on Disruptions, MHD, and I. P. B. Editors, *Nucl. Fusion* **39**, 2251 (1999).
- <sup>3</sup>S. Putvinski, P. Barabaschi, N. Fujisawa, N. Putvinskaya, M. N. Rosenbluth, and J. Wesley, *Plasma Phys. Controlled Fusion* **39**, B157 (1997).
- <sup>4</sup>H.-W. Bartels, *Fusion Eng. Des.* **23**, 323 (1993).
- <sup>5</sup>M. Shimada, D. J. Campbell, V. Mukhovatov, M. Fujiwara, N. Kirneva, K. Lackner, M. Nagami, V. D. Pustovitov, N. Uckan, J. Wesley, N. Asakura, A. E. Costley, A. J. H. Donné, E. J. Doyle, A. Fasoli, C. Gormezano, Y. Gribov, O. Gruber, T. C. Hender, W. Houlberg, S. Ide, Y. Kamada, A. Leonard, B. Lipschultz, A. Loarte, K. Miyamoto, V. Mukhovatov, T. H. Osborne, A. Polevoi, and A. C. C. Sips, *Nucl. Fusion* **47**, S1 (2007).
- <sup>6</sup>T. Hender, J. C. Wesley, J. Bialek, A. Bondeson, A. H. Boozer, R. J. Buttery, A. Garofalo, T. P. Goodman, R. S. Granetz, Y. Gribov, O. Gruber, M. Gryaznevich, G. Giruzzi, S. Günter, N. Hayashi, P. Helander, C. C. Hegna, D. F. Howell, D. A. Humphreys, G. T. A. Huysmans, A. W. Hyatt, A. Isayama, S. C. Jardin, Y. Kawano, A. Kellman, C. Kessel, H. R. Koslowski, R. J. La Haye, E. Lazzaro, Y. Q. Liu, V. Lukash, J. Manickam, S. Medvedev, V. Mertens, S. V. Mirnov, Y. Nakamura, G. Navratil, M. Okabayashi, T. Ozeki, R. Paccagnella, G. Pautasso, F. Porcelli, V. D. Pustovitov, V. Riccardo, M. Sato, O. Sauter, M. J. Schaffer, M. Shimada, P. Sonato, E. J. Strait, M. Sugihara, M. Takechi, A. D. Turnbull, E. Westerhof, D. G. Whyte, R. Yoshino, H. Zohm, and The ITPA MHD,

- Disruption and Magnetic Control Topical Group, *Nucl. Fusion* **47**, S128 (2007).
- <sup>7</sup>R. Nygren, T. Lutz, D. Walsh, G. Martin, M. Chatelier, T. Loarer, and D. Guilhem, *J. Nucl. Mater.* **241–243**, 522 (1997).
  - <sup>8</sup>S. Jardin, G. L. Schmidt, E. D. Fredrickson, K. W. Hill, J. Hyun, B. J. Merrill, and R. Sayer, *Nucl. Fusion* **40**, 923 (2000).
  - <sup>9</sup>K. Finken, G. Mank, A. Krämer-Flecken, and R. Jaspers, *Nucl. Fusion* **41**, 1651 (2001).
  - <sup>10</sup>D. Whyte, T. C. Jernigan, D. A. Humphreys, A. W. Hyatt, C. J. Lasnier, P. B. Parks, T. E. Evans, M. N. Rosenbluth, P. L. Taylor, A. G. Kellman, D. S. Gray, E. M. Hollmann, and S. K. Combs, *Phys. Rev. Lett.* **89**, 055001 (2002).
  - <sup>11</sup>M. Lehnen, S. A. Bozhkov, S. S. Abdullaev, M. W. Jakubowski, and TEXTOR Team, *Phys. Rev. Lett.* **100**, 255003 (2008).
  - <sup>12</sup>R. Jaspers, N. J. Lopes Cardozo, K. H. Finken, B. C. Schokker, G. Mank, G. Fuchs, and F. C. Schüller, *Phys. Rev. Lett.* **72**, 4093 (1993).
  - <sup>13</sup>V. Plyusnin, V. Riccardo, R. Jaspers, B. Alper, V. G. Kiptily, J. Mlynar, S. Popovichev, E. de La Luna, F. Andersson, and JET EFDA Contributors, *Nucl. Fusion* **46**, 277 (2006).
  - <sup>14</sup>R. Gill, *Nucl. Fusion* **33**, 1613 (1993).
  - <sup>15</sup>B. Esposito, J. R. Martín-Solís, F. M. Poli, J. A. Mier, R. Sánchez, and L. Panaccione, *Phys. Plasmas* **10**, 2350/11 (2003).
  - <sup>16</sup>T. Kawamura, H. Obayashi, and A. Miyahara, *Fusion Eng. Des.* **9**, 45 (1989).
  - <sup>17</sup>T. Kudyakov, K. H. Finken, M. W. Jakubowski, M. Lehnen, Y. Xu, B. Schweer, T. Toncian, G. van Wassenhove, O. Willi, and the TEXTOR team, *Nucl. Fusion* **48**, 122002 (2008).
  - <sup>18</sup>M. Forster, K. H. Finken, M. Lehnen, J. Linke, B. Schweer, C. Thomser, O. Willi, Y. Xu, and the TEXTOR team, *Nucl. Fusion* **51**, 043003 (8pp) (2011).
  - <sup>19</sup>T. Kudyakov, A. Jochmann, K. Zeil, S. Kraft, K. H. Finken, U. Schramm, and O. Willi, *Rev. Sci. Instrum.* **80**, 076106 (2009).
  - <sup>20</sup>A. Loarte, V. Riccardo, J. R. Martín-Solís, J. Paley, A. Huber, M. Lehnen, and JET EFDA Contributors, *Nucl. Fusion* **51**, 073004 (20pp) (2011).
  - <sup>21</sup>M. Forster, K. H. Finken, M. Lehnen, O. Willi, Y. Xu, and the TEXTOR Team, *Phys. Plasmas* **19**, 052506 (2012).
  - <sup>22</sup>H. M. Smith, T. Fehér, T. Fülöp, K. Gál, and E. Verwichte, *Plasma Phys. Controlled Fusion* **51**, 124008 (2009).
  - <sup>23</sup>M. Forster, S. S. Abdullaev, K. H. Finken, T. Kudyakov, M. Lehnen, G. Sewell, O. Willi, Y. Xu, and the TEXTOR Team, “Runaway electron transport in turbulent and resonantly perturbed magnetic topologies of TEXTOR,” *Nucl. Fusion* **52**, 083016 (13pp) (2012).